

NASA

Technical Memorandum 79199

AVRADCOM

Technical Report 80-C-4

SIMPLIFIED FATIGUE LIFE ANALYSIS  
FOR TRACTION DRIVE CONTACTS

(NASA-TM-79199) SIMPLIFIED FATIGUE LIFE  
ANALYSIS FOR TRACTION DRIVE CONTACTS (NASA)  
30 p HC A03/MF A01 CSCL 13I

N80-17469

Unclas  
G3/37 47105

Douglas A. Rohn and Stuart H. Loewenthal  
Lewis Research Center

and

John J. Coy  
Propulsion Laboratory  
AVRADCOM Research and Technology Laboratories  
Lewis Research Center  
Cleveland, Ohio

Prepared for the  
Third International Power Transmission and Gearing Conference  
sponsored by the American Society of Mechanical Engineers  
San Francisco, California, August 18-22, 1980

# **SIMPLIFIED FATIGUE LIFE ANALYSIS FOR TRACTION DRIVE CONTACTS**

by Douglas A. Rohn, Stuart H. Loewenthal

Lewis Research Center

and

John J. Coy

Propulsion Laboratory

AVRADCOM Research and Technology Laboratories

Lewis Research Center

Cleveland, Ohio

## **ABSTRACT**

A simplified fatigue life analysis for traction drive contacts of arbitrary geometry is presented. The analysis is based on the Lundberg-Palmgren theory used for rolling-element bearings. The effects of torque, element size, speed, contact ellipse ratio, and the influence of traction coefficient are shown. The analysis shows that within the limits of the available traction coefficient, traction contacts exhibit longest life at high speeds. Multiple, load-sharing roller arrangements have an advantageous effect on system life, torque capacity, power-to-weight ratio and size.

## **INTRODUCTION**

The development of practical, cost-competitive traction drives for a variety of commercial applications, from machine tools to automotive transmissions, is a rapidly expanding field. Although presently about a dozen companies in the United States market variable speed traction drives [1], their widest acceptance has been in Europe, where thousands are in commercial service. Interest is also remarkably high in Japan and the Soviet Union. The majority of these commercial drives are limited to light-duty applications, less than 11 kW (15 hp) [1]. However, progress is being made in developing higher power capacity drives by using cleaner vacuum-processed bearing steels with greater fatigue resistance and traction lubricants with improved tractive properties [2].

When designing or selecting a traction drive, one must be concerned with the service life of the unit. Presently, very little fatigue life data is available from well controlled traction contact fatigue tests. However, many investigations have been conducted on rolling-element fatigue for rolling element bearings [3]. Due to the similarity

in the expected failure mode, namely, rolling-element fatigue, the life analysis methods used to establish rolling-element bearing capacity ratings should be applicable to determining the service life and capacity of traction drive contacts [4].

The purpose of this investigation is to simplify the traction drive fatigue analysis presented in [4], derived from Lundberg-Palmgren theory [5], and to use this analysis to study the effects of rotational speed, power level, contact ellipticity ratio, multiplicity of contacts and variation in the available traction coefficient on traction drive contact stresses, system life, size and power capacity. Design charts are to be provided for determining the 90-percent survival life rating of steel, traction drive contacts of arbitrary geometry. References to material, lubrication and traction life modifying factors will be made.

## ANALYSIS

### Fatigue Life Model

In 1947 Lundberg and Palmgren [5] published a statistical theory for the failure distribution of ball and roller bearings. The mode of failure was assumed to be subsurface-originated (SSO) fatigue pitting. Lundberg and Palmgren theorized that SSO fatigue pitting was due to high stresses in the neighborhood of a stress-raising incongruity in the bearing material.

The theory is used by bearing manufacturers to establish rolling-element bearing fatigue life ratings. In references [6,7] the theory was applied to predicting the fatigue life of spur and helical gears. The predicted life of a steel gear set was confirmed with life data from full scale spur gear tests [7]. The theory has also been adapted to analyzing the fatigue lives of traction drives [4].

For a steel rolling-element, the number of stress cycles endured before failure occurs is given by the following equation [4]:

$$L = \left( \frac{K_1 z_o^h}{\tau_o^c V} \right)^{1/e} \quad (1)$$

This equation is a modified form of the Lundberg-Palmgren theory for contact-fatigue life prediction and is applicable to gears, bearings, and other rolling-contact elements.

The critical shear stress,  $\tau_0$ , is considered to be the maximum orthogonal reversing shear stress which occurs below the surface of the contacting elements. This stress is not the largest of the subsurface stresses but has the largest fluctuating component which is critical to the fatigue process. The stressed volume term,  $V$ , is important since Lundberg-Palmgren theory is based on the probability of encountering a fatigue initiating flaw in the volume of the material that is being stressed. The depth to the critical stress,  $z_0$ , is a relative measure of the distance the fatigue crack must travel in order to emerge at the surface and thus cause failure. For rolling-element bearings (and bodies in rolling-contact in general) made of AISI 52100 steel, Rockwell-C 62 hardness, with a fatigue life at a 90-percent probability of survival, the following values are appropriate for use in equation (1) to determine life in millions of stress cycles:

$$\begin{aligned} K_1 &= 1.430 \times 10^{95} \text{ (N and m units)} \\ &= 3.583 \times 10^{56} \text{ (lbf and in. units)} \end{aligned}$$

Based on life tests of ball and roller bearings, the accepted exponent values are  $h = 7/3$ ,  $c = 31/3$ , and  $e = 10/9$  for elliptical shape point contact or  $e = 3/2$  for line contact [5].

### Contact Stress Analysis

The stress analysis of elastic bodies in contact was developed by H. Hertz [8]. Hertz assumed homogeneous solid elastic bodies made of isotropic material which are characterized by Young's modulus  $E$  and Poisson's ratio  $\xi$ . Bodies A and B in contact are assumed to have quadratic surfaces in the neighborhood of the contact point. The theory of Hertz is summarized by Harris [9]. A simplified presentation will be used here for the purpose of developing a life formula.

Figure 1 shows two bodies in contact. Planes  $x$  and  $y$  are the respective planes of maximum and minimum relative curvature for the bodies. These planes, are mutually perpendicular. They are also perpendicular to the plane which is tangent to the contacting bodies surfaces at the point of contact. Planes  $x$  and  $y$  must be chosen so that the relative curvature in plane  $x$  is greater than in plane  $y$ , thus:

$$\frac{1}{r_{Ax}} + \frac{1}{r_{Bx}} > \frac{1}{r_{Ay}} + \frac{1}{r_{By}} \quad (2)$$

The radii of curvature may be positive or negative depending on whether the surfaces are convex or concave, respectively.

When the bodies are pressed together, the point of contact is assumed to flatten into a small area of contact which is bounded by an ellipse with major axis  $2a$  and minor axis  $2b$  as shown in Fig. 1. Plane  $y$  contains the major axis of the contact ellipse and plane  $x$  contains the minor axis. The ratio  $a/b$  is called the ellipticity ratio of the contact. The values of  $a/b$  range from 1 to  $\infty$  for various curvature combinations of contacting surfaces. For cylinders in contact, the ellipticity ratio approaches  $\infty$ , and the flattened area of contact is a rectangular strip. For spheres in contact the ellipticity ratio is 1. The first type is called line contact and all other types are called point contact.

When performing contact analysis, one must be aware of the geometrical orientation of the rolling radii, crown radii, and principal planes. In some traction drive contacts, the principal radii  $r_{Ax}$  and  $r_{Bx}$  of equation (2), as shown in Fig. 1, are equal to the contacting element rolling radii, and radii  $r_{Ax}$  and  $r_{By}$  are equal to the transverse or crown radii or vice versa. However, the principal radii for drive contacts using tapered rollers or those in toroidal drives are generally not equal to the rolling radii or its orthogonal component since these radii are not normal to the surface at the point of contact. The principal radii for use in this analysis must always lie in planes that are perpendicular to the contact plane.

The maximum surface contact pressure at the center of the elliptical pressure distribution is

$$\sigma_o = \frac{3Q}{2\pi ab} \quad (3)$$

where the semimajor and semiminor contact ellipse axes are:

$$a = a^*g \quad (4)$$

$$b = b^*g \quad (5)$$

and the auxiliary contact size parameter is:

$$g = \sqrt[3]{\frac{3Q}{2\rho} \left( \frac{1 - \xi_A^2}{E_A} + \frac{1 - \xi_B^2}{E_B} \right)} \quad (6)$$

and where the inverse curvature sum is:

$$\rho = \frac{1}{r_{Ax}} + \frac{1}{r_{Bx}} + \frac{1}{r_{Ay}} + \frac{1}{r_{By}} \quad (7)$$

For steel contacting bodies, with  $E_A = E_B = 207 \text{ GPa}$  ( $3.0 \times 10^7 \text{ psi}$ ) and  $\xi_A = \xi_B = 0.3$ , the auxiliary contact size parameter can be expressed as:

$$g = 2.36 \times 10^{-4} \sqrt[3]{\frac{Q}{\rho}} \quad (\text{N and m units})$$

or

$$g = 4.50 \times 10^{-3} \sqrt[3]{\frac{Q}{\rho}} \quad (\text{lbf and in. units})$$

The values of  $a^*$  and  $b^*$ , the dimensionless contact ellipse semimajor and semiminor axes, can be determined from the elliptical integrals used in Hertzian theory [9]. Figure 2 from [9] shows  $a^*$  and  $b^*$  plotted as a function of the relative curvature difference,  $F$ , where

$$F = \frac{\frac{1}{r_{Ax}} + \frac{1}{r_{Bx}} - \left( \frac{1}{r_{Ay}} + \frac{1}{r_{By}} \right)}{\rho} \quad (8)$$

The magnitude of the critical stress, that is, the subsurface maximum orthogonal reversing shear stress  $\tau_o$  and its depth  $z_o$  in equation (1) are also functions of  $F$ . These parameters can be found in Fig. 3 from [9] in terms of  $2\tau_o/\sigma_o$  and  $z_o/b$  as functions of  $F$ . Also needed for equation (1) is the stressed volume  $V$  which for a rolling-element contact is given by:

$$V = az_o 2\pi R$$

where  $R$  is the element's rolling radius. Thus, the term  $2\pi R$  is equal to the length of the rolling track which is traversed during one revolution.

#### Fatigue Life Equation

**Elliptical contacts.** - Estimation of the theoretical fatigue life of a rolling-element contact based on the aforementioned equations and figures is fairly straightforward. However, for a traction drive with many contacts the calculations can become tedious and the relationship between life and contact size, shape, and load is unclear. By

substituting the previously discussed terms into equation (1), a simpler formula can be developed, which expresses the life in terms of material constants, applied load, and contacting body geometry.

By using Fig. 3 and equations (3) and (5) to find  $\tau_o$  and  $z_o$ , and using equations (4) and (9) to find  $V$ , the important parameters of equation (1) can be found. Assuming both contacting bodies are of the same material (i.e.,  $E_A = E_B$  and  $\xi_A = \xi_B$ ) and using the exponents and material factor already given, the substitution results in the following:

$$L = K_3(K_2)^{9/10} [Q^{-10/3} (E' \rho)^{-7} |R|^{-1}]^{9/10} \quad (10)$$

where

$L$  = 90-percent survival life of a single contacting element in millions of stress cycles

$$\begin{aligned} K_3 &= 8.18 \times 10^{90} \text{ (N and m units)} \\ &= 1.49 \times 10^{56} \text{ (lbf and in. units)} \end{aligned}$$

$$K_2 = \left( \frac{z_o}{b} \right)^{4/3} \left( \frac{\tau_o}{\sigma_o} \right)^{31/3} (a^*)^{28/3} (b^*)^{35/3} \quad (11)$$

$$E' = \frac{E}{1 - \xi^2} \quad (12)$$

and where  $R$  is the rolling radius of the body. If the contacting bodies are steel, with  $E = 207 \text{ GPa}$  ( $3.0 \times 10^7 \text{ psi}$ ) and  $\xi = 0.3$ , then equation (10) becomes:

$$L = K_4(K_2)^{0.9} Q^{-3} \rho^{-6.3} |R|^{-0.9} \quad (13)$$

where

$$\begin{aligned} K_4 &= 2.32 \times 10^{19} \text{ (N and m units)} \\ &= 6.43 \times 10^8 \text{ (lbf and in. units)} \end{aligned}$$

The variable  $K_2$  in equations (10) and (13) contains four factors, each of which depend only on  $F$ , the relative curvature difference. From the values of  $a^*$  and  $b^*$  shown in Fig. 2 one can determine that the contact ellipticity ratio  $a/b$  is also a function of  $F$ . Thus, given either  $F$  or  $a/b$ , the variable  $K_2$  can be determined as shown in Fig. 4.

Equation (13) is valid for the most common contacts where the contact ellipse is oriented such that the semimajor axis is perpendicular to the direction of rolling. As shown in Fig. 1, this is the case when rolling occurs in the  $x$  direction. If this is the case and the rolling radii are also equal to the principal radii, that is  $R_A = r_{Ax}$  and  $R_B = r_{Bx}$ , then

$$\rho = \frac{2}{R_A} \left( \frac{1 + \frac{R_A}{R_B}}{1 + F} \right) \quad (14)$$

and from equation (13)

$$L = K_5 (K_2)^{0.9} Q^{-3} \left( \frac{1 + \frac{R_A}{R_B}}{1 + F} \right)^{-6.3} |R_A|^{5.4} \quad (15)$$

where

$$\begin{aligned} K_5 &= 2.95 \times 10^{17} \text{ (N and m units)} \\ &= 8.16 \times 10^6 \text{ (lbf and in. units)} \end{aligned}$$

and where  $R_A$  is the rolling radius of the body whose life in millions of stress cycles is  $L$  and  $R_B$  is the rolling radius of the mating body.

To this point, the contact ellipse semimajor axis has been assumed to be oriented perpendicular to the direction of rolling. However, if the principal planes are chosen such that rolling occurs in the  $y$  direction, then the semiminor axis is perpendicular to the rolling direction. For a contact under these latter conditions, the stressed volume expression, equation (9), must contain the semiminor axis,  $b$ , instead of the semimajor axis,  $a$ . Equations (10) to (13) are still valid with the exception that in equation (11) the exponent on  $a^*$  becomes  $25/3$  and the exponent on  $b^*$  becomes  $32/3$ .

An expression for the maximum surface contact pressure can also be developed for steel bodies from equations (6) to (9) where:



$$\left. \begin{aligned} \sigma_o &= \frac{8.55 \times 10^6}{a^* b^*} Q^{1/3} \rho^{2/3} \text{ (N and m units)} \\ \sigma_o &= \frac{2.36 \times 10^4}{a^* b^*} Q^{1/3} \rho^{2/3} \text{ (lbf and in. units)} \end{aligned} \right\} \quad (16)$$

or

Line contacts. - The analysis presented thus far has been confined to point contact. In the case of line contact, it can be shown that

$$L = K_6 Q^{-3} |R_A|^{3.22} W^{2.33} \left( 1 + \frac{R_A}{R_B} \right)^{-3.89} \quad (17)$$

where

$$\begin{aligned} K_6 &= 4.21 \times 10^{25} \text{ (N and in. units)} \\ &= 6.71 \times 10^{14} \text{ (lbf and in. units)} \end{aligned}$$

and where  $R_A$  is the rolling radius of the body whose life, in millions of stress cycles, is  $L$ , and  $R_B$  is the rolling radius of the mating body.

The expression for maximum surface contact pressure in line contact is

$$\sigma_o \propto Q^{1/2}$$

and therefore from equation (17)

$$L \propto \sigma_o^{-6}$$

However, the sixth power relationship between fatigue life and contact pressure is unlike that of any rolling-contact fatigue data known to the authors. Most data shows at least a ninth power relationship [10]. In [7] fatigue tests on spur gears, whose contact geometry approximates that of a line contact, life was inversely related to the 8.6 power of stress. Additionally the Lundberg-Palmgren data which was used to establish the line contact exponents was generated for a roller bearing which assumed a "modified" line contact. This contact was analytically developed from an elliptical contact stress distribution which had been mathematically corrected [5]. Furthermore, it is not desirable to design traction contacts without some transverse curvature. Transverse curvature is required to avoid the adverse effects of excessive edge loading

as a result of possible axis skew, misalignment or overhang. In view of the above, the life equation for line contact should be used with discretion.

**System life.** - Heretofore, the equations express rolling-element fatigue life for a single rolling-element in terms of millions of stress cycles. However, in the case of a traction drive, it is system life that is important. All bodies in a system accumulate stress cycles at different rates because their speeds of rotation and number of stress cycles per revolution may not all be the same. In order to compare lives of the various bodies clock time should be used. Assume that the speed in revolutions per minute of the  $i^{\text{th}}$  body is  $n_i$  and that there are  $u_i$  stress cycles per revolution, then the life of body  $i$  in hours is given by:

$$H_i = \frac{L_i}{u_i n_i} \frac{10^6}{60} \quad (18)$$

The life of the system is then found by applying Weibull's rule [9]. If the system consists of  $j$  roll bodies and the life of each is designated  $H_i (i = 1 \text{ to } j)$ , then the system life in hours is given by:

$$H_s = \left[ \frac{1}{(H_1)^e} + \frac{1}{(H_2)^e} + \dots + \frac{1}{(H_j)^e} \right]^{-1/e} \quad (19)$$

Thus for the simplest arrangement, a single pair of rollers, the contact life in hours for an elliptical contact would be

$$H_s = \left[ \frac{1}{(H_1)^{10/9}} + \frac{1}{(H_2)^{10/9}} \right]^{-9/10}$$

where  $e = 10/9$  and  $H_1$  and  $H_2$  are equal to the individual lives of each roller.

**Size effects.** - It is evident from equation (13) that for a given rolling-contact, increasing the load will decrease life by a power of 3, in addition, a direct relationship exists between life and element size (radius and contact width). For constant torque and traction coefficient,  $Q \propto 1/R$ . For constant relative radii difference,  $F$ , the transverse radius or contact width is proportional to the rolling radius. Therefore,  $\text{size} \propto R$ . Also,  $K_2 = \text{constant}$  and  $\rho \propto R$ . Substituting these proportionalities into

equation (13) and noting that size and rolling radius can be interchanged yields:

$$L \propto \left( \frac{1}{\text{size}} \right)^{-3} \left( \frac{1}{\text{size}} \right)^{-6.3} (\text{size})^{-0.9}$$

or

$$L \propto (\text{size})^{8.4}$$

#### Life Adjustment Factors

Advancements in rolling-element bearing technology since the publication of the Lundberg-Palmgren theory have generally increased bearing fatigue lives. These improvements resulted from the use of improved materials and manufacturing techniques along with a better understanding of the variables affecting fatigue life. In recognition of these advancements, life adjustment factors have been developed [3] for adjusting Lundberg-Palmgren fatigue life ratings for ball and roller bearings. Several of these factors are considered to be equally applicable to traction drive elements in view of the similarities in contact geometry, operating conditions, failure modes, materials and lubrication [4]. The factors which are appropriate are the material, processing and lubrication factors. An additional factor, not considered for rolling-element bearings in [3], but important to traction drive contacts is the potentially deleterious effect which traction may have on fatigue life. The addition of a tangential force component to the contact will alter the subsurface stress field which may in turn change the fatigue life. Some investigators [11] have found a decrease in life from rolling element fatigue tests when relative sliding and traction are introduced. Rolling-element fatigue tests [12] with increased spin (i.e., rotational sliding within the contact area) also showed a reduction in fatigue life. However, insufficient data currently exists to properly quantify the effects of traction on rolling-element fatigue life.

In this present analysis, these life adjustment factors are not considered. Comparisons are made on the basis of the unmodified theoretical predictions. Application of the analysis developed herein to an actual traction drive should include the life adjustment factors published in [3].

## RESULTS AND DISCUSSION

### Effect of Roller Speed and Geometry

To illustrate the effects of some of the parameters in equation (13) on relative life, a parametric study was conducted. Some typical traction drive contact configurations were used. Rollers of different size, speed, number, and contact ellipticity ratio were investigated. The relative effects of roller size and speed on drive system is of interest to the designer of traction drive systems. Generally, for a given power level and life, the size of a power transmitting element, such as a gear or a traction drive roller, can be reduced as speed is increased since torque decreases.

Size and speed effects. - Figure 5(a) shows the effects of size and speed on relative contact life for an arbitrary pair of crowned rollers of constant  $a/b$  and ratio, operating at a given power level under a fixed applied traction coefficient,  $\mu^*$ . As would be expected, an increase in size increases life. Increasing the operating speed accumulates more stress cycles per hour, but since the speed and torque are inversely related for constant power, the decrease in torque and thus normal load is more significant. This results in longer life at higher speeds. More importantly, Fig. 5(a) shows that for a constant life condition, the rolling traction element size can be reduced with increased rotational speed.

Figure 5(a) was generated for a constant applied traction coefficient  $\mu^*$ . However, traction data [13, 14] for various lubricants show that the maximum available traction coefficient  $\mu$  decreases with an increase in surface speed and with a decrease in contact pressure. Typical traction data from a twin disk machine described in [14] is given in Fig. 6 where the maximum available traction coefficient  $\mu$  is plotted versus surface speed for various maximum contact pressures and a contact ellipse ratio of 5. To provide a safe margin against gross slippage, 75 percent of this maximum coefficient is used in the calculations.

An arbitrary pair of crowned rollers of constant ratio and  $a/b$  of 5 operating at a given power level were again analyzed for fatigue life. The contacting rollers were assumed to operate with the highest possible traction coefficient based on the data of Fig. 6. The appropriate value of  $\mu$  to use in this comparison was found from an

iterative process since  $\mu$  is dependent on the contact pressure and speed and vice versa.

Figure 5(b) shows once again, that an increase in size and speed increases fatigue life. The reason for higher life in either the constant  $\mu$  or variable  $\mu$  case is that increasing a traction roller's size or rotational speed for constant power reduces the tangential force and thus the normal load and contact pressure. However, reducing the contact pressure or increasing the surface speed produces a loss of available traction coefficient and thus a need for a higher normal load in order to transmit the torque. This loss in  $\mu$  causes a flattening of the life trend with increased speed as shown in Fig. 5(b). In fact, for the range shown, the life curve of the 1.5x and 2x size rollers reaches a maximum with speed and then diminishes, indicating an optimum speed for best life.

Ellipticity ratio effects. - Traction contact life is also influenced by the relative curvatures of the bodies. For a typical pair of traction rollers for constant normal load, speed, and rolling radii, varying the transverse radii can have a large effect on the estimated fatigue life. Figure 7 illustrates the results of a sample calculation. It is evident from Fig. 7, that an increase in  $a/b$  will increase the area of contact and cause a corresponding decrease in contact pressure with an attendant improvement in life. However this effect is somewhat diminished when the loss in the available traction coefficient due to the decrease in contact pressure is taken into account. Furthermore contacts with large value of  $a/b$  tend to have lower values of  $\mu$  under spin and higher spin losses.

#### Effect of Multiple Contacts on Capacity and Life

Weight and size efficient traction drives [15-19] generally require multiple, load sharing contacts. The extent that multiple, parallel contacts reduce unit loading, improve life and power capacity can easily be explored with the analysis presented here. The basic configurations to be investigated are a set of multiple identical "planet" rollers in external contact with a central "sun" roller and a set of multiple identical "planet" rollers in internal contact with a "ring" roller. These arrangements typify the multiple contacts that can be found in many types of traction drives [1]. For a given roller speed ratio, there exists a maximum number of planet rollers which will

fit around the sun or within the ring without interference. Figure 8 details these maxima.

By beginning with a simple two roller contact, carrying a certain torque, a multiple roller cluster is formed by adding additional rollers without changing speed, roller size and sun or ring torque. The life increase and contact pressure decrease for multiple roller contacts as shown in Fig. 9. Due to the parallel paths, each element is loaded in proportion to the inverse of the number of planets in the cluster. However life is not proportional to the cube of the number of planets as equation (13) alone would indicate because the system life decreases with an increase in the number of components according to equation (19) and the sun or ring experience more stress cycles per revolution with more planets. Figure 9 is valid for both external and internal contact configurations of any size, ratio, and allowable number of rollers for constant torque, traction coefficient, ellipticity ratio and element size. An expression for the life as a function of number of planets can be derived from equation (13) and is given in Fig. 9. A sample calculation for a three planet external contact configuration using equation (13) is shown in Table I.

Another advantage of the multiple contact geometry is the relative compactness of such a traction drive assembly. Figure 10 shows the relative cluster diameter and contact pressure versus number of multiple planet rollers for both external and internal configurations of any ratio operating under constant sun or ring torque conditions at equal system fatigue life. The relative cluster diameter is defined as the ring roller bore diameter or as the pitch diameter of the planet rollers in the case of the sun arrangement. The effect of planet number on the relative sun or ring torque capacity of a certain cluster package size is illustrated in Fig. 11, for constant size, ratio, traction coefficient and fatigue life in both external and internal contact arrangements.

Figures 9, 10, and 11 show that, for a given application, the maximum number of multiple, load sharing rollers possible within geometrical ratio limits is advantageous to fatigue life, drive size and torque capacity. Multiple, load sharing planets also effect the relative power-to-weight ratio of a set of traction elements. The relative power-to-weight ratio increases, with an increase in the numbers of external planets

for a constant system life and diameter as shown in Fig. 12. In Fig. 12, the relative power is obtained from Fig. 11 and the relative weight is determined from the number of planets and their volumes. In calculating the respective system weight the width of the rolling track varied with the contact ellipse width. The lines of constant sun-to-planet radius ratio plotted in Fig. 12 were chosen as the minimum ratio allowable for 4, 5, 6, 8, 10, and 12 planets as shown in Fig. 8.

### SUMMARY OF RESULTS

A simplified calculation method for predicting the rolling-element fatigue life of traction drive systems with elliptical contacts was developed. A modified form of the Lundberg-Palmgren theory is used as the basis of this fatigue life model. This life model considers stress, stressed volume and depth to the critical shear stress as well as the effect of multiple contacting elements. The method was applied to a simple pair of rolling element traction bodies transmitting a constant power level over a range of element sizes, rotational speeds, and contact ellipticity ratios. The effects of available traction coefficient as a function of contact pressure and surface speed was also investigated.

The method was also applied to systems of multiple, load sharing rollers in external (sun) and internal (ring) contact arrangements. The system fatigue life for the multiple roller systems was computed for a range of system sizes, number of rollers, and ratios while the torque and traction coefficient were held constant. The following results were obtained.

1. Traction drive size, life, torque capacity per unit size and power-to-weight ratio improves with an increase in number of multiple load sharing rollers.
2. For a given power and size, the fatigue life of a traction contact increases with an increase in speed. However, an optimum speed exists, beyond which the loss in traction coefficient causes a loss in life.
3. The size of traction drive elements carrying a given power for a specified fatigue life decreases with an increase in rotating speed.

### SYMBOLS

- a contact ellipse semimajor axis, m (in.)
- a\* dimensionless contact ellipse semimajor axis
- b contact ellipse semiminor axis, m (in.)

$b^*$	dimensionless contact ellipse semiminor axis
$c$	orthogonal shear stress exponent
$E$	modulus of elasticity, Pa (psi)
$E'$	material elasticity parameter, Pa (psi)
$e$	Weibull exponent
$F$	relative curvature difference
$g$	auxiliary elliptical contact size parameter, m (in.)
$H$	drive system life, hr
$h$	depth to critical stress exponent
$K_1$	material constant
$K_2$	geometric life variable
$L$	life, millions of stress cycles
$N$	number of planet rollers
$n$	speed of rotation, rpm
$Q$	rolling body normal load, N (lbf)
$R$	rolling radius, m (in.)
$r$	radius, m (in.)
$u$	number of stress cycles per revolution
$V$	stressed volume, $m^3$ ( $in^3$ )
$W$	roller width, m (in.)
$z_0$	depth to critical stress, m (in.)
$\mu$	traction coefficient
$\mu^*$	applied traction coefficient
$\xi$	Poisson's ratio
$\rho$	inverse curvature sum, $m^{-1}$ ( $in^{-1}$ )
$\sigma_0$	maximum surface contact pressure, Pa (psi)
$\tau_0$	maximum reversing orthogonal shear stress, Pa (psi)

**Subscripts:**

$A, B$	elastic bodies
$i$	system element
$s$	system
$x, y$	reference planes

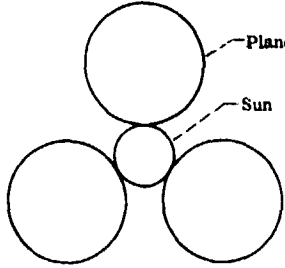


## REFERENCES

1. Carson, Robert W., "Traction Drives Update," Power Transmission Design, Vol. 19, No. 11, Nov. 1977, pp. 37-42.
2. Green, R. L., and Langenfeld, F. L., "Lubricants for Traction Drives," Machine Design, Vol. 46, No. 11, May 2, 1974, pp. 108-113.
3. Bamberger, E. N., et al., Life Adjustment Factors for Ball and Roller Bearings - An Engineering Guide, American Society of Mechanical Engineers, New York, 1971.
4. Coy, J. J., Loewenthal, S. H., and Zaretsky, E. V., "Fatigue Life Analysis for Traction Drives with Application to a Toroidal Geometry," NASA TN D-8362, 1976.
5. Lundberg, G. and Palmgren, A., "Dynamic Capacity of Rolling Bearings," Ingenioersvetenskapsakademien, Handlingar, No. 196, 1947.
6. Coy, J. J., Townsend, D. P., and Zaretsky, E. V., "Dynamic Capacity and Surface Fatigue Life for Spur and Helical Gears," Journal of Lubrication Technology, Vol. 98, No. 2, Apr. 1976, pp. 267-276.
7. Townsend, D. P., Coy, J. J., and Zaretsky, E. V., "Experimental and Analytical Load-Life Relation for AISI 9310 Steel Spur Gears," Journal of Mechanical Design, Vol. 100, No. 1, January 1978, pp. 54-60.
8. Hertz, H., Miscellaneous Papers, Part V - The Contact of Elastic Solids, The MacMillan Company (London), 1896, pp. 146-162.
9. Harris, T. A., Rolling Bearing Analysis, Wiley, New York, 1966.
10. Parker, R. J., Zaretsky, E. V., and Bamberger, E. N., "Evaluation of Load-Life Relation with Ball Bearings at 500° F," Journal of Lubrication Technology, Vol. 96, No. 3, July 1974, pp. 391-397.
11. MacPherson, P. B., "The Pitting Performance of Hardened Steels," ASME Paper No. 77-DET 39, Sep. 1977.
12. Zaretsky, E. V., Anderson, W. J., and Parker, R. J., "The Effect of Contact Angle on Rolling-Contact Fatigue and Bearing Load Capacity," ASLE Transactions, Vol. 5, 1962, pp. 210-219.

13. Hewko, L. O., Rounds, F. G., Jr., and Scott, R. L., 'Tractive Capacity and Efficiency of Rolling Contacts," Rolling Contact Phenomena, J. B. Bidwell, ed., Elsevier, Amsterdam, 1962, pp. 157-185.
14. Tevaarwerk, J. L., "Shear Behaviour of Elastohydrodynamic Oil Films," Proceedings of the Royal Society, London, Series A, Vol. 356, No. 1685, Aug. 24, 1977, pp. 215-236.
15. Nasvytis, A. L., "Multiroller Planetary Friction Drives," SAE Paper No. 660763, Oct. 1966.
16. Hewko, L. O., "Roller Traction Drive Unit for Extremely Quiet Power Transmission," Journal of Hydronautics, Vol. 2, No. 3, July 1968, pp. 160-167.
17. Loewenthal, S. H., Anderson, N. E., and Nasvytis, A. L., "Performance of a Nasvytis Multiroller Traction Drive," NASA TP-1378, 1978.
18. Nakamura, K., et al., "A Development of a Traction Roller System for a Gas Turbine Driven APU," SAE Paper No. 790106, Feb. 1979.
19. Loewenthal, S. H., Anderson, N. E., and Rohn, D. A., "Evaluation of a High Performance, Fixed-Ratio Traction Drive," proposed paper for the 1980 ASME International Power Transmission and Gearing Conference, August 1980.

TABLE 1. - SAMPLE CALCULATIONS

<p>Arrangement: External, three load sharing rollers</p> <p>Sun diameter, mm: 25</p> <p>Planet diameter, mm: 50</p> <p>Load, each contact, N: 1000</p> <p>Sun speed, rpm: 10 000</p> <p>Transverse radii, sun, mm: 500</p> <p>Transverse radii, planets, mm: 100</p>			
			
Parameter	Symbol	Formula	Result
Normal load, each contact, N	Q	-----	1000
Orthogonal principal radii, m	$r_{Ax}$	$\left\{ \begin{array}{l} \text{Must satisfy:} \\ \frac{1}{r_{Ax}} + \frac{1}{r_{Bx}} > \frac{1}{r_{Ay}} + \frac{1}{r_{By}} \end{array} \right\}$	0.0125
	$r_{Ay}$		0.5
	$r_{Bx}$		0.025
	$r_{By}$		0.1
Inverse curvature sum, $m^{-1}$	$\rho$	$\frac{1}{r_{Ax}} + \frac{1}{r_{Ay}} + \frac{1}{r_{Bx}} + \frac{1}{r_{By}}$	132
Relative curvature difference	F	$\frac{\frac{1}{r_{Ax}} + \frac{1}{r_{Bx}} - \left( \frac{1}{r_{Ay}} + \frac{1}{r_{By}} \right)}{\rho}$	0.818
Geometric life variable	$K_2$	Fig. 4	$1.65 \times 10^6$
Sun rolling radius, m	$R_{sun}$	-----	0.0125
Sun life, millions of cycles	$L_{sun}$	$K_4(K_2)^{0.9} Q^{-3} \rho^{-6.3} R_{sun}^{-0.9}$	$2.07 \times 10^4$
Sun stress, cycles/rev	$u_{sun}$	-----	3
Sun speed, rpm	$n_{sun}$	-----	10 000
Sun life, hr	$H_{sun}$	$\left( \frac{L}{u_{sun}} \right)_{sun} \left( \frac{10^6}{60} \right)$	11 500
Planet rolling radius, m	$R_{pl}$	-----	0.025
Planet life, millions of cycles	$L_{pl}$	$K_4(K_2)^{0.9} Q^{-3} \rho^{-6.3} R_{pl}^{-0.9}$	$1.11 \times 10^4$
Planet stress, cycles/rev	$u_{pl}$	-----	1
Planet speed, rpm	$n_{pl}$	-----	5000
Planet life, hr	$H_{pl}$	$\left( \frac{L}{u_{pl}} \right)_{pl} \left( \frac{10^6}{60} \right)$	37 000
System life, hr (without adjustment factors)	$H_s$	$\left[ \left( \frac{1}{H_{sun}} \right)^{10/9} + 3 \left( \frac{1}{H_{pl}} \right)^{10/9} \right]^{-9/10}$	6700

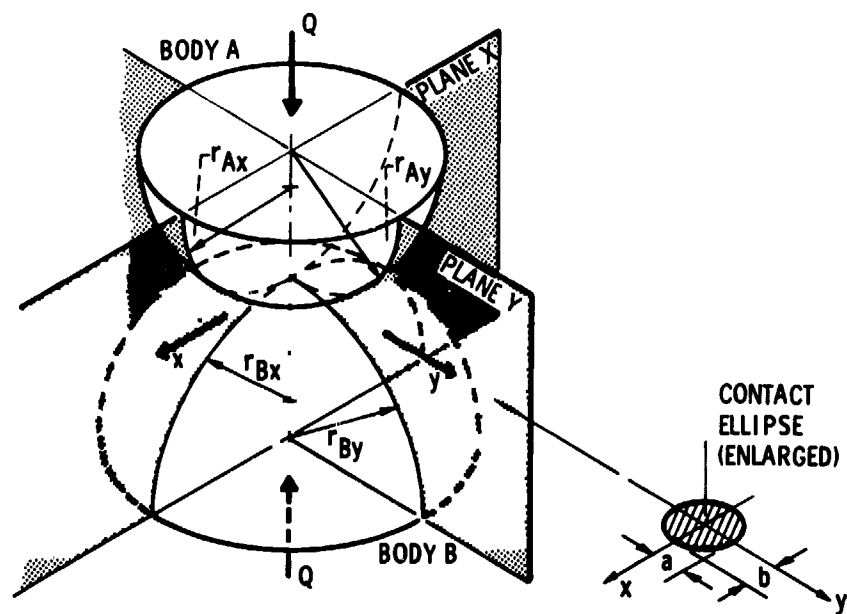


Figure 1. - Geometry of contacting solid elastic bodies.

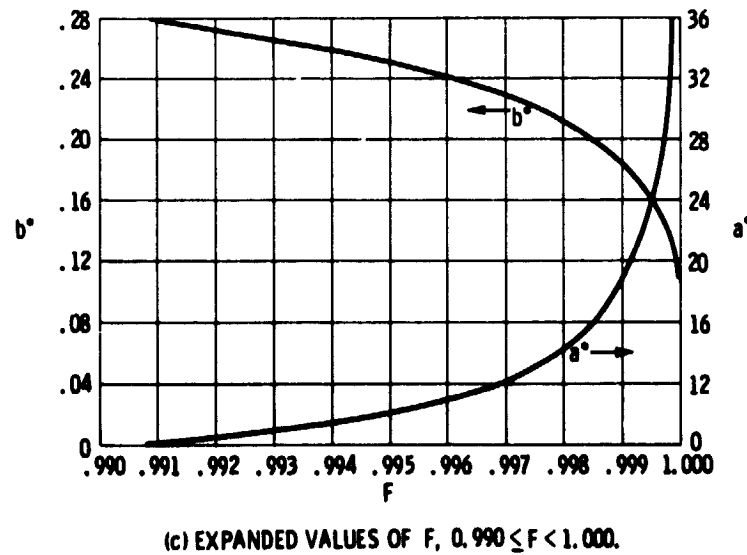
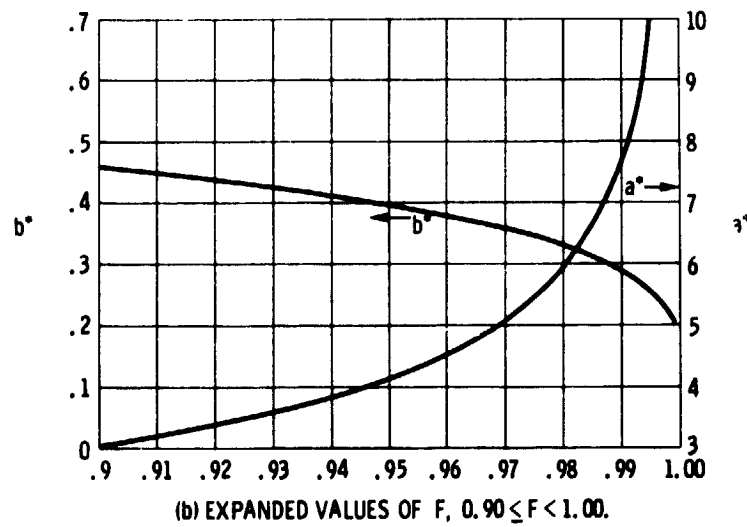
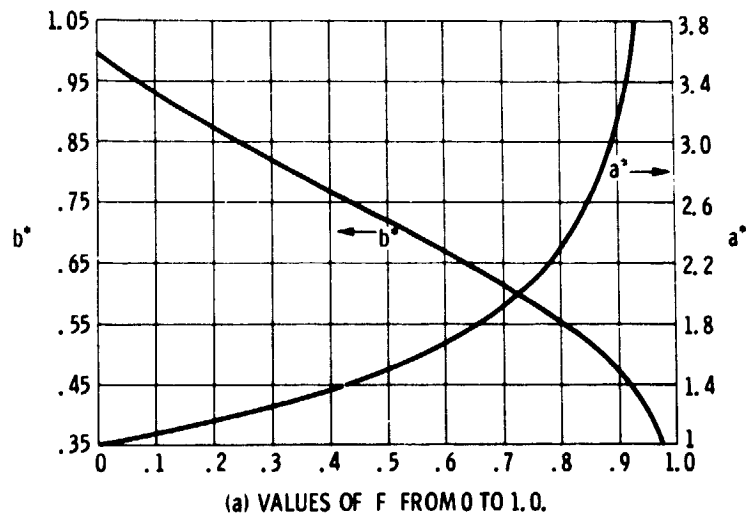


Figure 2. - Dimensionless elliptical contact semi-axes  $a^*$  and  $b^*$  vs. relative curvature difference from (9).

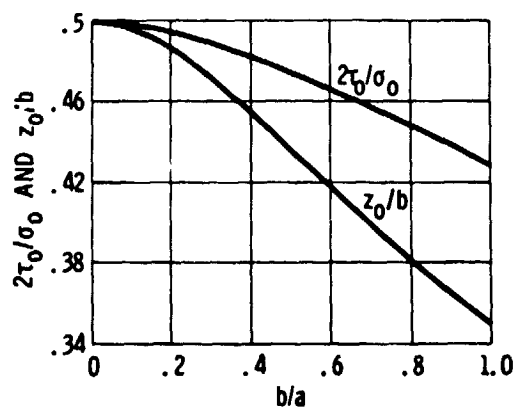


Figure 3.  $-2\tau_0/\sigma_0$  and  $z_0/b$  vs.  $b/a$  from [9].

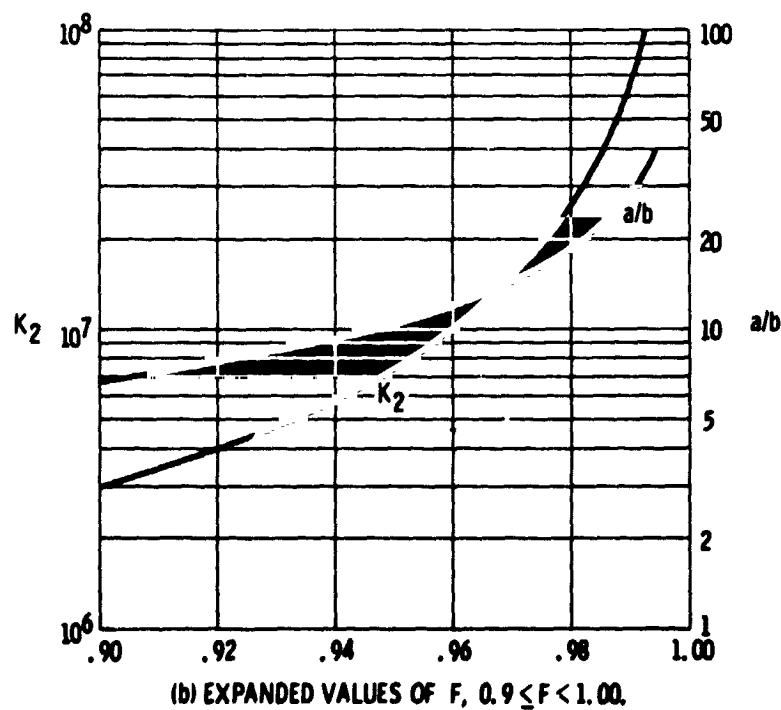
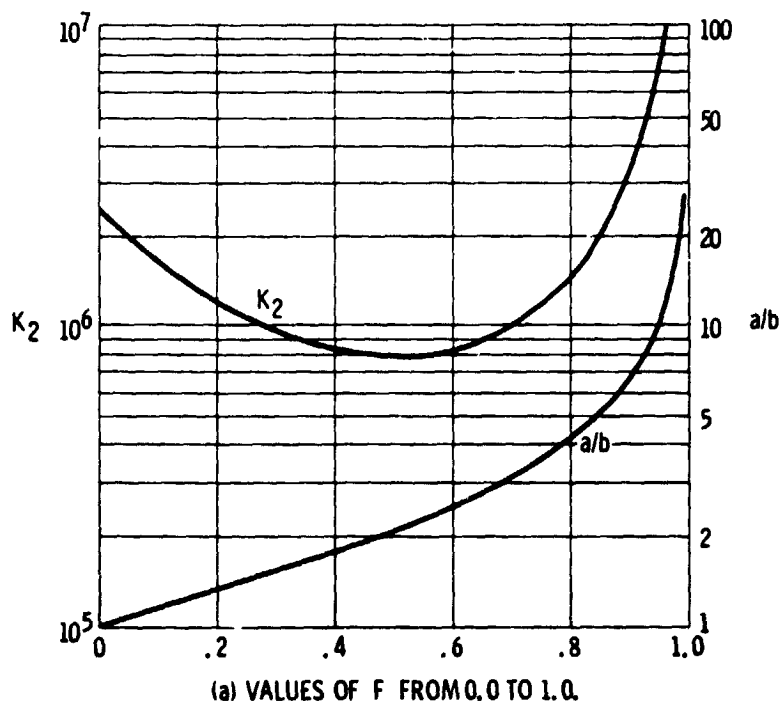
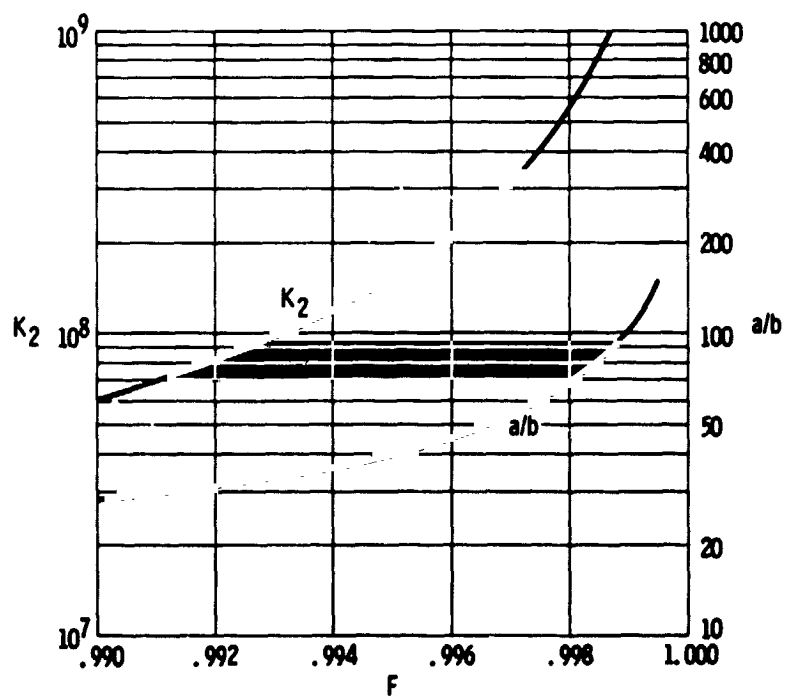


Figure 4. - Geometric life variable  $K_2$  and contact ellipticity ratio  $a/b$  vs. relative curvature difference,  $F$ .



(c) EXPANDED VALUES OF  $F$ ,  $0.99 \leq F < 1.000$ .

Figure 4. - Concluded.



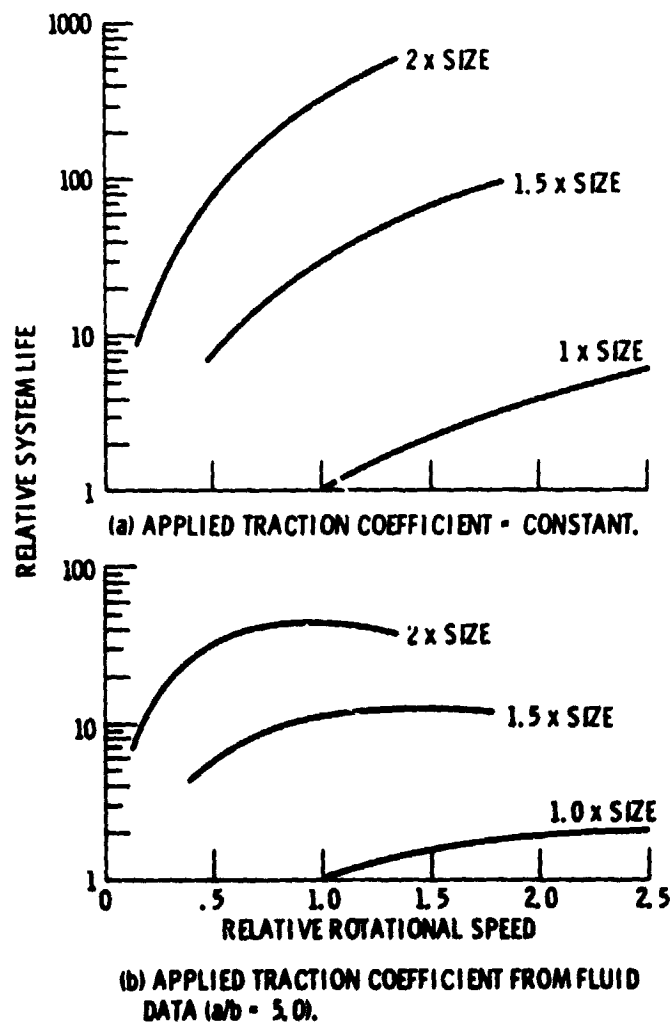


Figure 5. - Relative life vs. relative rotational speed for various size roller pairs in simple traction contact. Power, ratio, and  $a/b$  are constant.

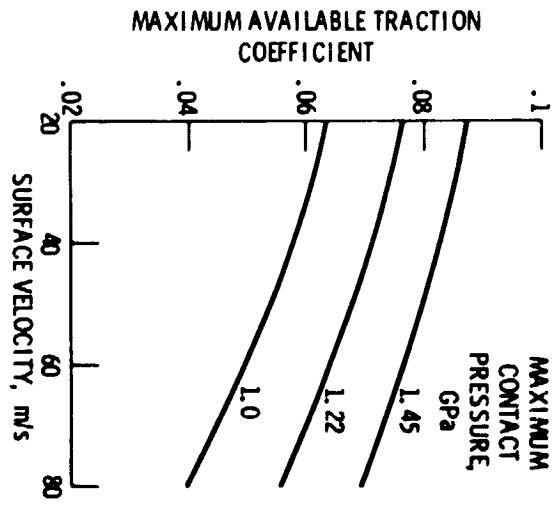


Figure 6. - Typical maximum available traction coefficient vs. surface velocity and maximum contact pressure. Synthetic hydrocarbon traction fluid,  $a/b = 5$ , zero spin, temperature = 343 K. From a twin disc machine described in [14].

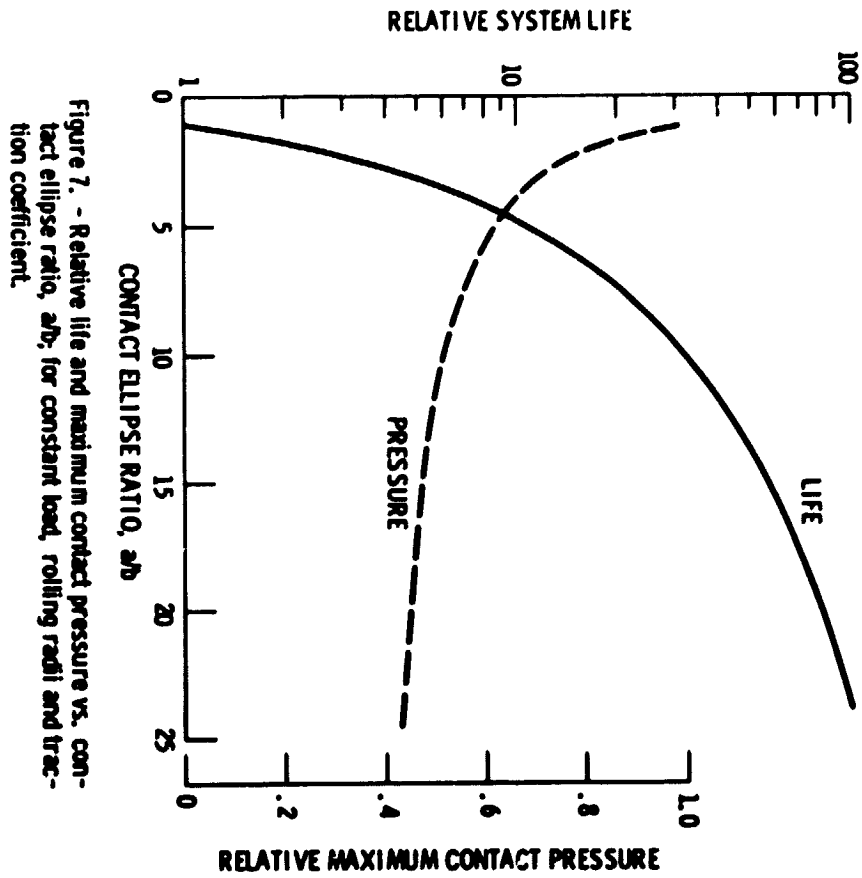


Figure 7. - Relative life and maximum contact pressure vs. contact ellipse ratio,  $a/b$ , for constant load, rolling radii and traction coefficient.

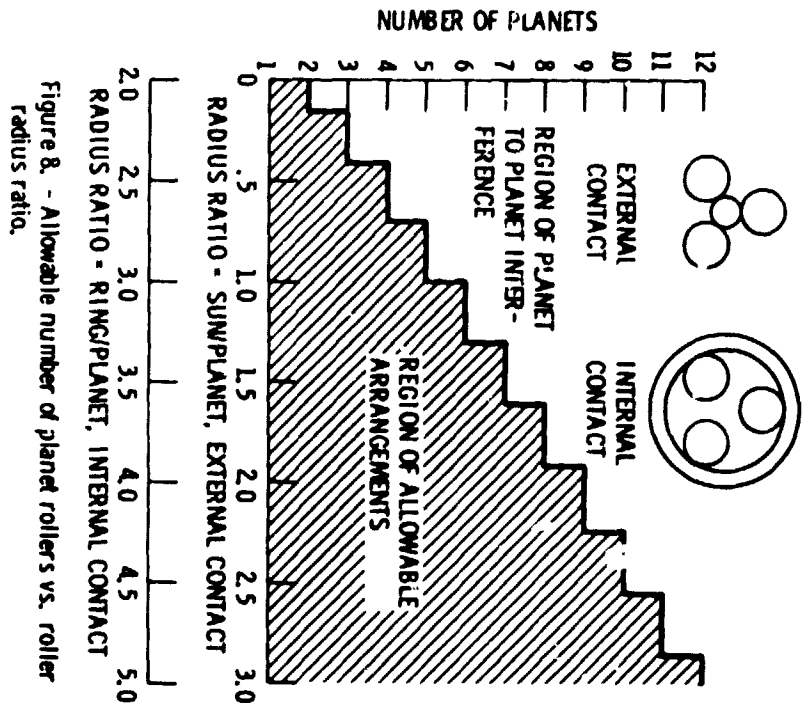


Figure 8. - Allowable number of planet rollers vs. roller radius ratio.

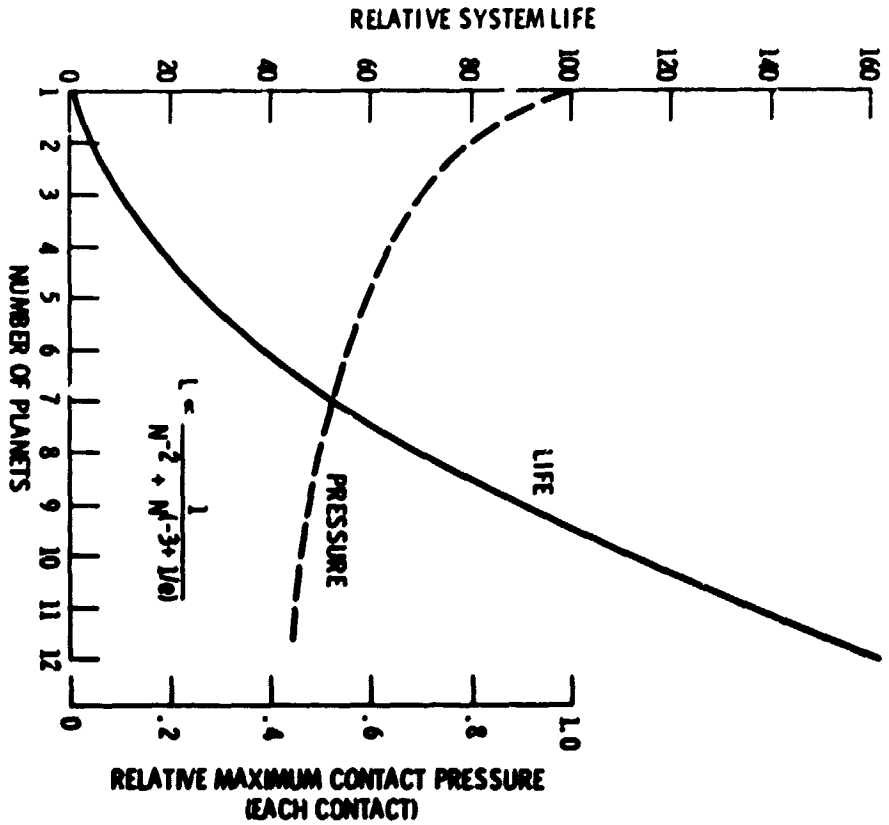


Figure 9. - Relative life and maximum contact pressure vs. number of planets for external or internal contact. Torque, element radii, and traction coefficient are constant.

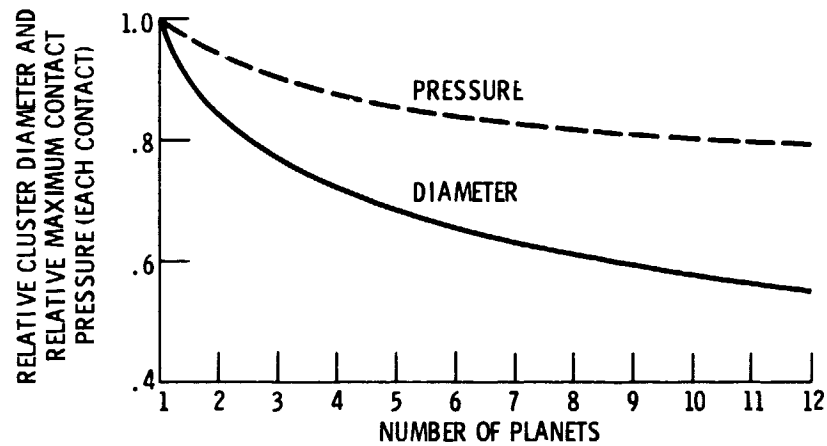


Figure 10. - Relative cluster diameter and relative maximum contact pressure vs. number of planets for external or internal contact. System life,  $a/b$  and torque are constant.

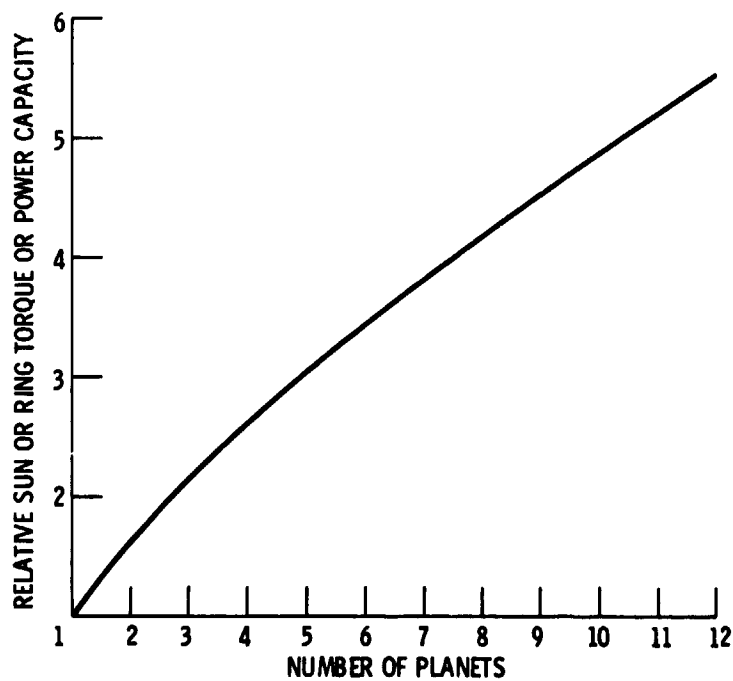


Figure 11. - Relative torque or power capacity vs. number of planets for external or internal contact. System life,  $a/b$  and rolling radii are constant.

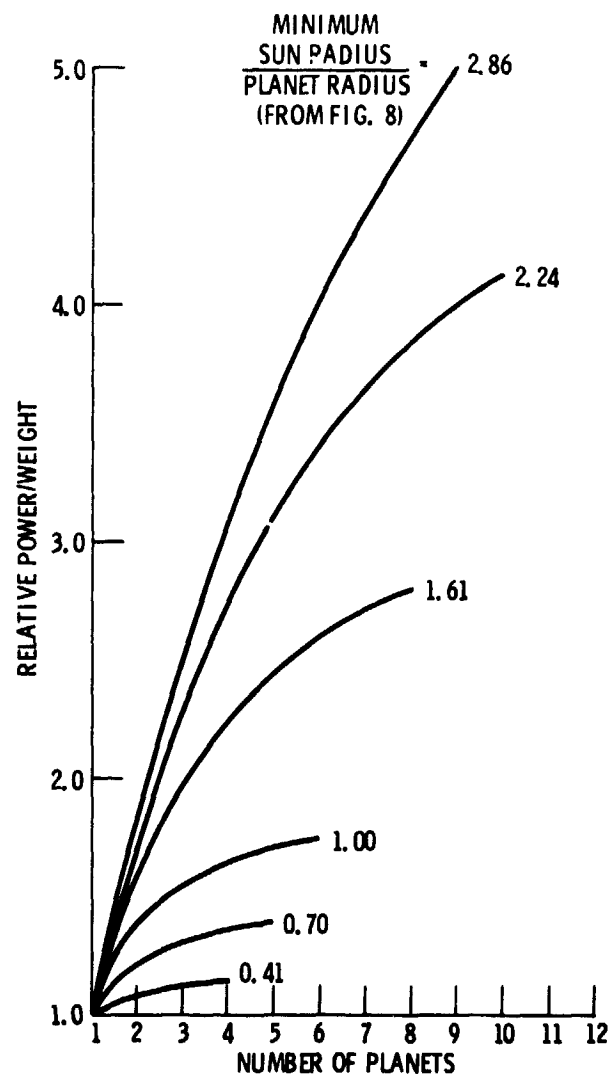


Figure 12. - Power-to-weight ratio vs. number of planets for external contact. System life, traction coefficient, rolling radii and  $a/b$  are constant. Roller width varies with contact ellipse major diameter.